ISAS - INTERNATIONAL SCHOOL FOR ADVANCED STUDIES

Thesis submitted for the degree

of

"MAGISTER PHILOSOPHIAE"

"APPROXIMATE QUANTUM-CLASSICAL SCHEMES FOR TUNNELING WITH COUPLING TO AN OSCILLATOR"

Candidate

Zhang Qiming

Supervisor

Prof. Erio Tosatti
Prof. A. Selloni

Academic Year 1986/87

TRIESTE

SISSA - SCUOLA INTERNAZIONALE SUPERIORE STUDI AVANZATI
TRIESTE
Strada Costiera 11

Approximate Quantum-Classical Schemes For Tunneling With Coupling To An Oscillator

Q. Zhang

International School for Advanced Study(SISSA), Trieste, Italy

* *This thesis is submitted for the degree of Magister of SISSA*

Content

Acknowledgements

This work has been carried out under the surpervision of Prof. E.Tosatti and Prof. A.Selloni. The auther wishes to thank them for not only their kind and patient guidances but also encouragement throughout the course of this study.

I. Introduction

The systems studied by condensed matter physics generally consist of an enormous number of electrons and nuclei. Solving the Schrodinger equation for such systems analytically is impossible, whereas numerical solutions by means of computers, although possible in principle, are inaccessible in practice. Approximations have to be done. The most essential and most widely used one is the Born-Oppenheimer(BO) adiabatic separation of electronic and nuclear motion [Bor27]. Since the electronic masses are so much lighter than those of the nuclei (or rigid ions sometimes), one may reasonably expect the electrons to follow the nuclear (or ionic) motion in a somehow adiabatic way. A slightly more general view is that the typical electronic excitation energies are so large on the scale of ionic frequency, that no electronic transition is induced by the ionic motion. If this is the case, the electronic energy eigenvalues can be treated as functions of the ionic coordinates and in turn contribute to the potential energy of the ions. In addition, if quantum features of the ionic motion do not play an important role in the problem, one can further use classical mechanics to describe it[Car86]. With this simplifications a large variety of problems become accessible.

However, the electronic energy levels which depend on the ionic coordinates may sometimes become very close to each other (on the scale of typical ionic frequencies). In these cases, a transition from one electronic state to the other might occur, and the electronic wavefunction might be

no longer an eigenstate of the Hamiltonian in which the ionic coordinates act as parameters. In this case, the adiabatic approximation itself breaks down, and hence the results obtained by the methods based on it become questionable. In the present thesis, we construct a model showing this kind of problem, investigate its dynamics by various approximate schemes and compare the results with the full quantum solution. Since the separation of electronic and ionic motion is a very convenient starting point for any approximate method, we hope to keep this separation and try to find some compensation to its failures.

In Section II, we present our model which consists of a particle (the "electron") which moves in an one-dimensional double-well potential and is coupled to an one-dimensional oscillator. We have chosen the parameters of our system so that the energy gap between the ground and first excited levels of the double-well subsystem at zero coupling is very small with respect to the oscillator frequency, whereas the higher levels are so far apart that they can be neglected. (The conditions for the validity of this approximation have been recently discussed in great detail by Leggett *et al.*[Leg87]) Within the BO approximation, electronic energy gap changes appreciably with the coordinate Q of the classical oscillator and becomes of the same order of the oscillator frequency. In section III, we present a fully quantum-mechanical, numerical solution of our model. Firstly, the system is calculated, then the dynamics is obtained for initial conditions which equivalent to those used in the following approximate calculations. In section IV, V and VI, several treatments which we call adiabatic, Ehrenfest and

trajectory surface hopping(TSH) schemes respectively are used to solve the model. This is done for three different values of the coupling constant. A comparison between the various results is presented in Section VII, together with our conclusions. They can be roughly summarized as follows:

1. The adiabatic evolution is generally the worst approximation to the true evolution.
2. The TSH method of Tully works best when the adiabatic potential energy surfaces have isolated near-crossing points (tunneling points), and keep well apart most of the time.
3. The Ehrenfest evolution is closest to the true evolution in the opposite situation of nearly parallel potential energy surfaces, with no well-defined near-crossing points.

II. Model

We want to simulate a situation in which two electronic levels come close to each other for some ionic configurations. In such a case the adiabatic approximation breaks down, because the electronic levels can come closer than the ionic, or vibrational levels. The simplest model exhibiting this features is perhaps a ("electron") system coupled to a harmonic oscillator. Analogous to what done by Leggett *et al.*[Let87], the two-state system is realized with a double-well which has a continuous degree of freedom q, just like Fig.1. The model Hamiltonian can be written as

$$H = -\frac{1}{2}\frac{d^2}{dq^2} + \frac{B}{4}q^4 - \frac{A}{2}q^2 - \frac{1}{2}\frac{d^2}{dQ^2} + \frac{1}{2}\omega_0^2 Q^2 + \lambda qQ \qquad (2.1)$$

$$\equiv T_q + V_e(q) + T_N + V_I(Q) + V_c(q,Q)$$

$$\equiv h(q;Q) + T_N + V_I(Q)$$

where A, B, ω_0 are arbitrary positive parameters to be chosen, $V_c = \lambda qQ$ is a coupling term and λ is a coupling constant. For convenience, we set the masses of both subsystem equal to unity. Throughout the thesis, we adopt atomic unit(a.u.). At appropriate parameters, we can obtain, for the q-subsystem, a very close energy level gap $\Delta = \varepsilon_1 - \varepsilon_0$ ($>> \omega_0$), whereas the other gaps $\Delta_i = \varepsilon_i - \varepsilon_1$ ($i \geq 2$) are much larger than ω_0. we can reasonably think that the motion of the q-subsystem is restricted to the lowest two states. If the q-subsystem is localized on one side of the double-well at the very beginning, it can tunnel to the other side with a period $2\pi/\Delta$. The motion of the two subsystem can have influence on each other through the coupling.

For the q-subsystem(λ=0), we would like to obtain a set of levels such that the lowest two are very close and the others are so high above that they can be neglected. In order to find the sequence of levels, we must solve the stationary state equation

$$[-\frac{1}{2}\frac{d^2}{dq^2} + V_e(q)]\ \varphi_i(q) = \varepsilon_i \varphi_i(q) \qquad (2.2)$$

The solution for this one-dimensional problem can be achieved by the numerical Runge-Kutta method, just like that done in atomic calculations [Her62] (more details will be given in section IV.). By choosing B=1 and A=4 the first few eigenvalues of Schrodinger equation are ε_0= -2.66145, ε_1=-2.65173 and ε_2=-0.51029, which give out an effective two-state system. The potential for this set of parameters is shown in Fig.1. The energy spectrum is plotted as well. In Fig.1, ε_0 and ε_1 are indistinguishable. Now we set the oscillator frequency ω_0 equal to 0.3, which is much higher than the gap Δ(= 0.009716) but much less than the gaps $\Delta_{i\geq 2}$(>2.0). Therefore we can indeed restrict our attention to just the lowest two levels of the q-subsystem[Leg87].

When the coupling to the oscillator is switched on, the level structure of the "electron" Hamiltonian at fixed Q, h(q;Q), is qualitatively unchanged. The spectra for different values of λ, as obtained by the method described in Sec.III, are shown in Fig.2. As a reference, we put the two subsystems' spectra (λ=0) on the left hand of the graph. For comparing convenience, the oscillator's levels are obtained from the potential $V(0,Q)+\varepsilon_0$, where ε_0 is the ground state of V(q,0). This implies that the zero point of energy

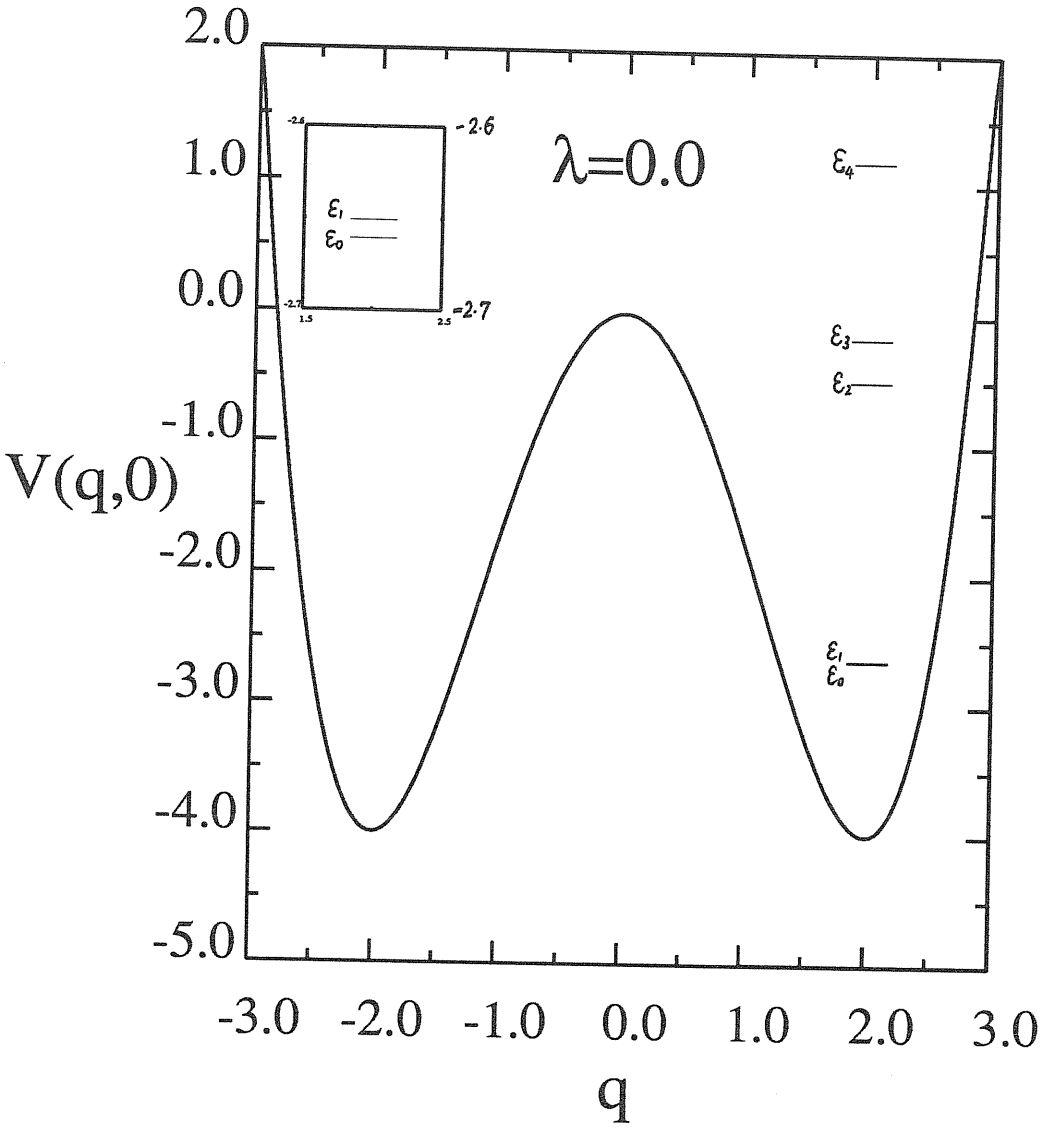

Fig.1 The potential of q-subsystem(λ=0). The levels are ploted as well. The lowest two are almost degenerate. Their fine structure is given at the top on the left.

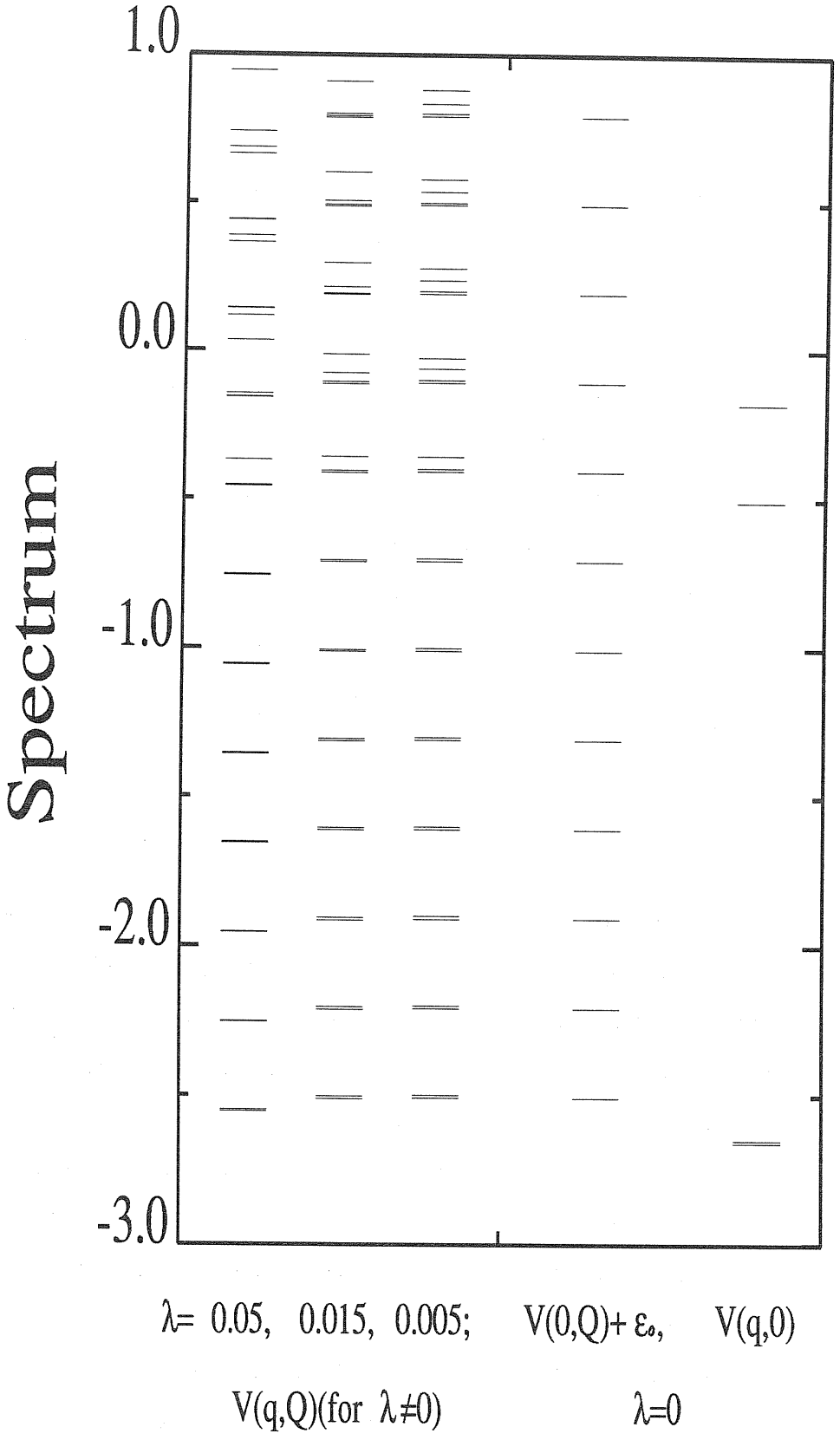

Fig.2 The spectra below 1.0 of the system for three values of λ. The spectra of two subsystems (λ=0) are given on the right hand side as the reference.

has been moved to ε_0. When λ approaches 0, the energy eigenvalues for the whole system can approximately be written as

$$E = e_m + \varepsilon_n \qquad (2.3)$$

where e_m is the energy eigenvalue of the oscillator. For a fixed e_m, there is a set of ε_n's. The second excited level is far above, hence most of the levels appear doublets. It is noticed that the larger the λ is, the closer these double levels are. At the same time they become deeper. This is because the distance between the two minima of $V(q,Q)$, D, equals to

$$D = \left(A + \frac{\lambda^2}{\omega_0^2} \right)\left(1 + \frac{\lambda^2}{\omega_0^4} \right) / B \qquad (2.4)$$

and the minimal value V_0 equals to

$$V_0 = -\frac{1}{4}\left(A + \frac{\lambda^2}{\omega_0^2} \right)^2 / B \qquad (2.5)$$

So when λ increases, D increases and V_0 decreases, implying that the doublet levels lend to become degenerate and shift downwards.

In the present thesis, three different values of λ have been used, i.e. λ=0.05, 0.015, 0.005. We set up our criterion for the strength of the coupling as follows: when the oscillator's potential energy surface (see Sec.IV) corresponding to the ground state of the electron appears to have two minima rather than one, then the coupling becomes strong. This is similar to the case studied by R. Graham and his co-workers[Gra84]. Fig.3 shows the potential energy surfaces of Q for different values of λ. They are weak, intermediate and strong cases respectively according to the criterion. It appears that the nonadiabatic transitions occur most probably at Q=0.0, especially in the strong coupling case.

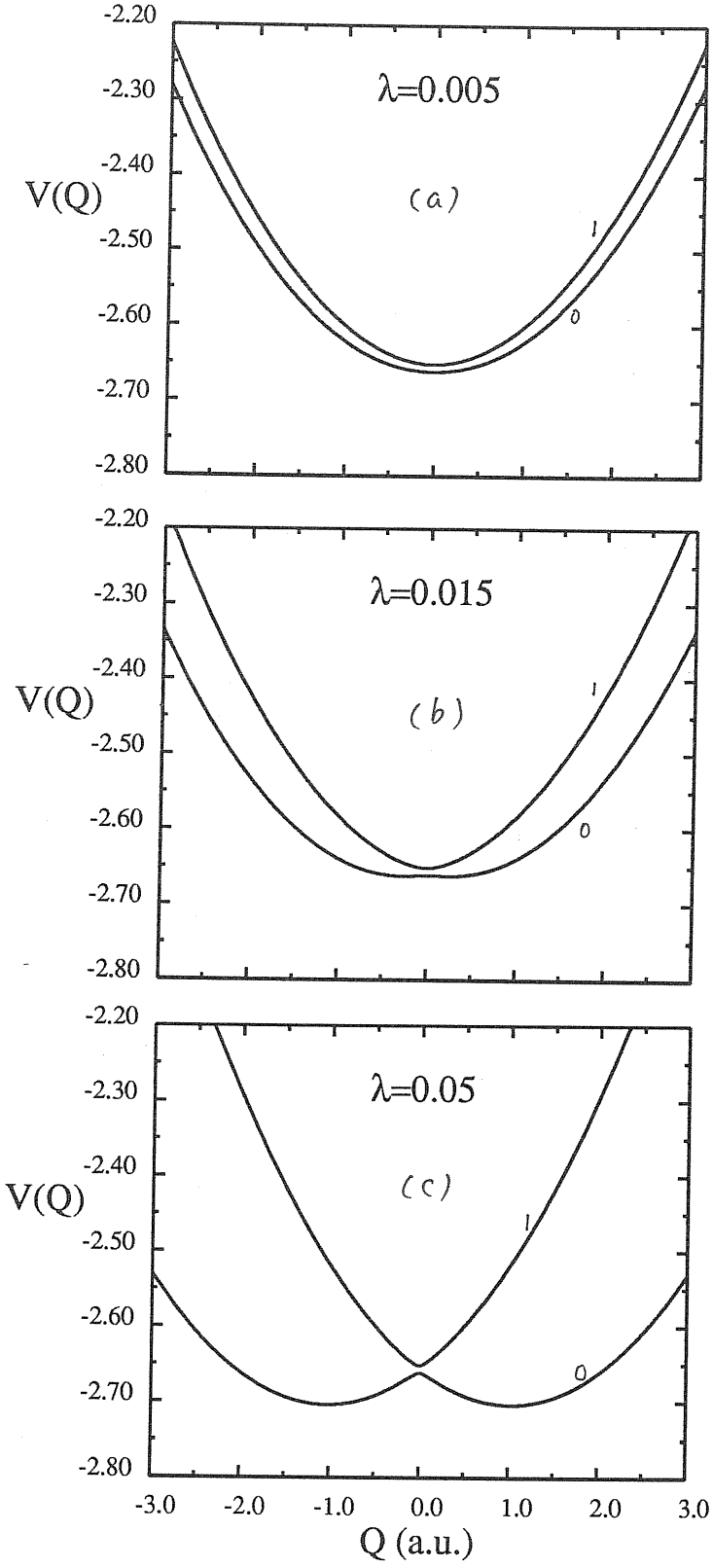

Fig.3 The potential energy surfaces of the oscillator for three different coupling constants: (a) weak, (b) intermediate and (c) strong.

III. Full Quantum Treatment

In this section, we solve the Schrodinger equation for the whole particle + oscillator system

$$H(q,Q)\Psi_i(q,Q)=E_i\Psi_i(q,Q) \qquad (3.1)$$

where the Hamiltonian $H(q,Q)$ is

$$H(q,Q)=-\frac{1}{2}\frac{d^2}{dq^2}-\frac{1}{2}\frac{d^2}{dQ^2}+V(q,Q) \qquad (3.2)$$

and $V(q,Q)$ is given in Eq.(2.1).

After having determined a set of eigenfunction, we shall calculate the time evolution of a given wave packet by expanding it on this basis.

a. Spectrum

The explicit stationary Schrodinger equation for our model is

$$[-\frac{1}{2}\frac{d^2}{dq^2}-\frac{1}{2}\frac{d^2}{dQ^2}+\frac{\beta}{4}q^4-\frac{A}{2}q^2+\frac{\omega_2^2}{2}Q+\lambda qQ]\Psi_i(q,Q)=E_i\Psi_i(q,Q) \qquad (3.3)$$

Since an analytic solution of Eq.(3.3) is not possible, we employ a matrix method to solve it. First of all, we need a set of basis functions to expand Ψ_i as

$$|\Psi_i\rangle=\sum_{mn} C_{mn}^{i}\,|m,n\rangle \qquad (3.4)$$

where the C_{mn}^{i}'s are the expansion coefficients, and the $|m,n\rangle$'s are the functions we are looking for. Because the potential consists of wells, it is natural to choose $|m,n\rangle$ as the direct product of two one-dimensional harmonic oscillators' eigenfunctions

$$|m,n\rangle=|m\rangle|n\rangle \qquad (3.5)$$

where $|m\rangle$ is the m-th eigenvector for the Q coordinate with

a frequency ω_Q and $|n\rangle$ is the n-th eigenvector for the q coordinate with a frequency ω_q. We choose ω_Q equal to the frequency of the oscillator of our model, i.e. $\omega_Q=\omega_o$, and ω_q equal to the square root of the 2nd-order expansion coefficient of V (q) (rf. Eq.(2.1)) at one of the bottoms of the double well. (In fact, we have found that the final results is to a large extent insensitive to the choice of ω_q.)

The Hamiltonian operators for these two oscillators are

$$h_a(q)=-\frac{1}{2}\frac{d^2}{dq^2}+\frac{1}{2}\omega_q^2 q^2=(a^\dagger a+\frac{1}{2})\omega \qquad (3.6)$$

$$h_b(Q)=-\frac{1}{2}\frac{d^2}{dQ^2}+\frac{1}{2}\omega_Q^2 Q=(b^\dagger b+\frac{1}{2})\omega \qquad (3.7)$$

respectively. Here $a^\dagger$, a, $b^\dagger$, b are creation and destruction operators for the two harmonic oscillators respectively.

Comparing Eqs.(3.6) and (3.7) with Eq.(3.2), the Hamiltonian for our model can be expressed as

$$H(q,Q)=h_a(q)+h_b(Q)+\frac{B}{4}q^4-\frac{1}{2}(A+\omega_q^2)q^2+\lambda qQ \qquad (3.8)$$

Substituting

$$q=\frac{1}{\sqrt{2\omega_q}}(a^\dagger+a) \qquad (3.9)$$

$$Q=\frac{1}{\sqrt{2\omega_Q}}(b^\dagger+b) \qquad (3.10)$$

into Eq.(3.8), we can get the matrix elements of h(q,Q) as

$$H_{m'n',mn}=\langle m',n'|H|m,n\rangle$$

$$=[(n+\tfrac{1}{2})\omega_q+(m+\tfrac{1}{2})\omega_Q+\frac{B}{16\omega_q^2}(6n^2+6n+3)-\frac{1}{4\omega_q}(A+\omega_q^2)(2n+1)]\delta_{m,m'}\delta_{n,n'}+$$

$$+\frac{1}{2\sqrt{\omega_q\omega_Q}}[\sqrt{m(n+1)}\,\delta_{m',m-1}\delta_{n',n+1}+\sqrt{(n+1)(m+1)}\,\delta_{m',m+1}\delta_{n',n+1}+\sqrt{n(m+1)}\,\delta_{m',m+1}\delta_{n',n-1}+$$

$$+\sqrt{mn}\,\delta_{m',m-1}\delta_{n',n-1}]+[\frac{B}{16\omega_q^2}(4n-2)\frac{(A+\omega_q^2)}{4\omega_q}]\sqrt{n(n-1)}\,\delta_{n',n-2}\delta_{m',m}+$$

$$+[\frac{B}{16\omega_q^2}(4n+6)-\frac{(A+\omega_q^2)}{4\omega_q}]\sqrt{n^2+3n+2}\,\delta_{n',n+2}\delta_{m',m}+$$

$$+\frac{B}{16\omega_q^2}[\sqrt{n(n-1)(n-2)(n-3)}\,\delta_{n',n-4}+$$

$$+\sqrt{(n+1)(n+2)(n+3)(n+4)}\ \delta_{n',n+4}]\,\delta_{m',m} \qquad (3.11)$$

Now the problem is reduced to a diagonalization of the Hamiltonian matrix (3.11). This is performed numerically by employing the standard routine package EISPACK[Gar77].

To get a convergent results for parameters A=4, B=1, $\omega_0=0.3$ and three λ values 0.05, 0.015, 0.005, we have used 30 $|m>$'s and 25 $|n>$'s, so that H is a 750x750 matrix.

Table 3.1

The first three levels for three different λ values. The corresponding gaps and tunneling period for the lowest levels are given also.

λ	E_0	E_1	E_2	$\Delta=E_1-E_0$	$T=2\pi/\Delta$
0.05	-2.55783	-2.55083	-2.25622	7.000×10^{-3}	897.6
0.015	-2.51559	-2.50615	-2.21537	9.435×10^{-3}	665.9
0.005	-2.51191	-2.50222	-2.21188	9.685×10^{-3}	648.8

The lowest three eigenvalues obtained for the different values of λ are shown in Table 3.1. The gap reduces with increasing λ. The reason is that the distance between the minima of the double well increases with λ. The difference between E_1 and E_0 is essentially equal to ω_0. The spectrums below 0 are shown in Fig.2 and have been discussed in Sec.II. The tunneling period in Table 3.1 has the following meaning: Let

$$\Phi(q,Q,t)=e^{-iE_0t}\Psi_0+e^{-iE_1t}\Psi_1$$

$$=e^{-iE_0t}[\Psi_0+e^{-i\Delta t}\Psi_1] \qquad (3.13)$$

be a state at time t. Due to the symmetry properties of our model, Ψ_0 and Ψ_1 are symmetric and antisymmetric wavefunctions respectively. Therefore the combination

$$\Psi_0 + \Psi_1 \qquad (3.14)$$

is located in one well, and the combination

$$\Psi_0 - \Psi_1 \qquad (3.15)$$

is located in another. When t=0, $\Phi(q,Q,0)$ has the form of Eq.(3.14), and when t=T, it has the form of Eq.(3.15)(within a phase factor). This implies that the system tunnels from one well to another with a period $T=2\pi/\Delta$.

b. Motion of a wave packet

Since in the next three sections we shall treat the Q-subsystem (oscillator) classically, we need to make the present full quantum solution comparable to those semiclassical results.

Thus we construct a state whose wavefunction in Q-direction possesses the form of a wave packet whose center of gravity oscillates with the period of the classical motion[Sch54]. At t=0, the wave packet centered at Q_0 with a oscillating period ω_Q can be written as

$$\Psi(q,Q,0)=(\frac{\omega_Q}{\pi})^{1/4} u_0(q;Q=Q_0)\, e^{-\frac{1}{2}\omega_Q(Q-Q_0)^2} \qquad (3.16)$$

where $u_0(q,Q=Q_0)$ is the ground state of $h(q,Q)$ in Eq.(2.1) with the parameter Q equal to Q_0.

The state $\Psi(q,Q,t)$ can be expanded in terms of stationary wavefunctions $\Psi_\ell(q,Q)$'s

$$\Psi(q,Q,t)=\sum_\ell A_\ell \Psi_\ell(q,Q)\, e^{-iE_\ell t} \qquad (3.17)$$

The A_ℓ's can be obtained from the initial condition Eq.(3.16). We have the equality

$$\sum_\ell A_\ell \Psi_\ell(q,Q)=(\frac{\omega_Q}{\pi})^{1/4} u_0(q,Q_0)\, e^{-\frac{1}{2}\omega_Q(Q-Q_0)^2} \qquad (3.18)$$

so

$$A_\ell=\langle\Psi_\ell(q,Q)\,|\,\Psi(q,Q,0)\rangle \qquad (3.19)$$

Substituting Eqs.(3.4) and (3.5) into Eq.(3.19), expanding

$$u_0(q,Q_0)=\sum_n d_n\phi_n(q) \qquad (3.20)$$

and denoting

$$\tilde{A}_m=\int\left(\frac{\omega_Q}{\pi}\right)^{1/4} e^{-\frac{1}{2}\omega_Q(Q-Q_0)^2}\varphi_m(Q)\,dQ \qquad (3.21)$$

where $\phi_n(q)$, $\varphi_m(Q)$ are explicit expressions of $|n\rangle$, $|m\rangle$ respectively. From Schiff's textbook[Sch55]

$$A_m=\frac{\omega_Q^{m/2}\,Q_0^m\,e^{-\frac{1}{4}\omega_Q Q_0^2}}{(2^m\,m!)^{1/2}} \qquad (3.23)$$

The d_n's can be obtained numerically.

In our calculation, 25 A_ℓ's are used ($\sum_\ell |A_\ell|^2$ is better than 0.9999). This number has been checked to be good enough to give convergent results in the time scale (τ=1400 a.u.) we studied.

We now discuss our results, which are presented in Figs.4a, 5a, 6a, 7a, 8a and 9a for the three different values of the coupling λ. Here we show the time evolution of the expectation values of Q and q which are given by

$$\langle Q(t)\rangle=\langle\psi|Q|\psi\rangle$$
$$=\sum_\ell A_\ell^2\frac{1}{\sqrt{2\omega_Q}}\sum_{mn}\left[C^\ell_{m+1,n}C^\ell_{mn}\sqrt{m+1}+C^\ell_{m-1,n}C^\ell_{mn}\sqrt{m}\right]+$$
$$+2\sum_{\substack{\ell=1\\ \ell'>\ell}}A_\ell A_{\ell'}\cos(E_\ell-E_{\ell'})t\cdot\sum_{mn}\frac{1}{\sqrt{2\omega_Q}}\left[C^{\ell'}_{m+1,n}C^\ell_{m,n}\sqrt{m+1}+C^{\ell'}_{m-1,n}C^\ell_{m,n}\sqrt{m}\right] \qquad (3.24)$$

$$\langle q(t)\rangle=\langle\psi|q|\psi\rangle$$
$$=\sum_\ell A_\ell^2\frac{1}{\sqrt{2\omega_q}}\sum_{mn}\left[C^\ell_{m,n+1}C^\ell_{m,n}\sqrt{n+1}+C^\ell_{m,n-1}C^\ell_{m,n}\sqrt{n}\right]+$$
$$+2\sum_{\substack{\ell=1\\ \ell'>\ell}}A_\ell A_{\ell'}\cos(E_\ell-E_{\ell'})t\cdot\sum_{mn}\frac{1}{\sqrt{2\omega_q}}\left[C^{\ell'}_{m,n+1}C^\ell_{mn}\sqrt{n+1}+C^{\ell'}_{m,n-1}C^\ell_{m,n}\sqrt{n}\right] \qquad (3.25)$$

The $\langle Q(t)\rangle$ of the strong coupling (λ=0.05, see Fig.4a) moves somehow strangely. The amplitude also oscillate between 0 and a finite value, indicating the energy transfer

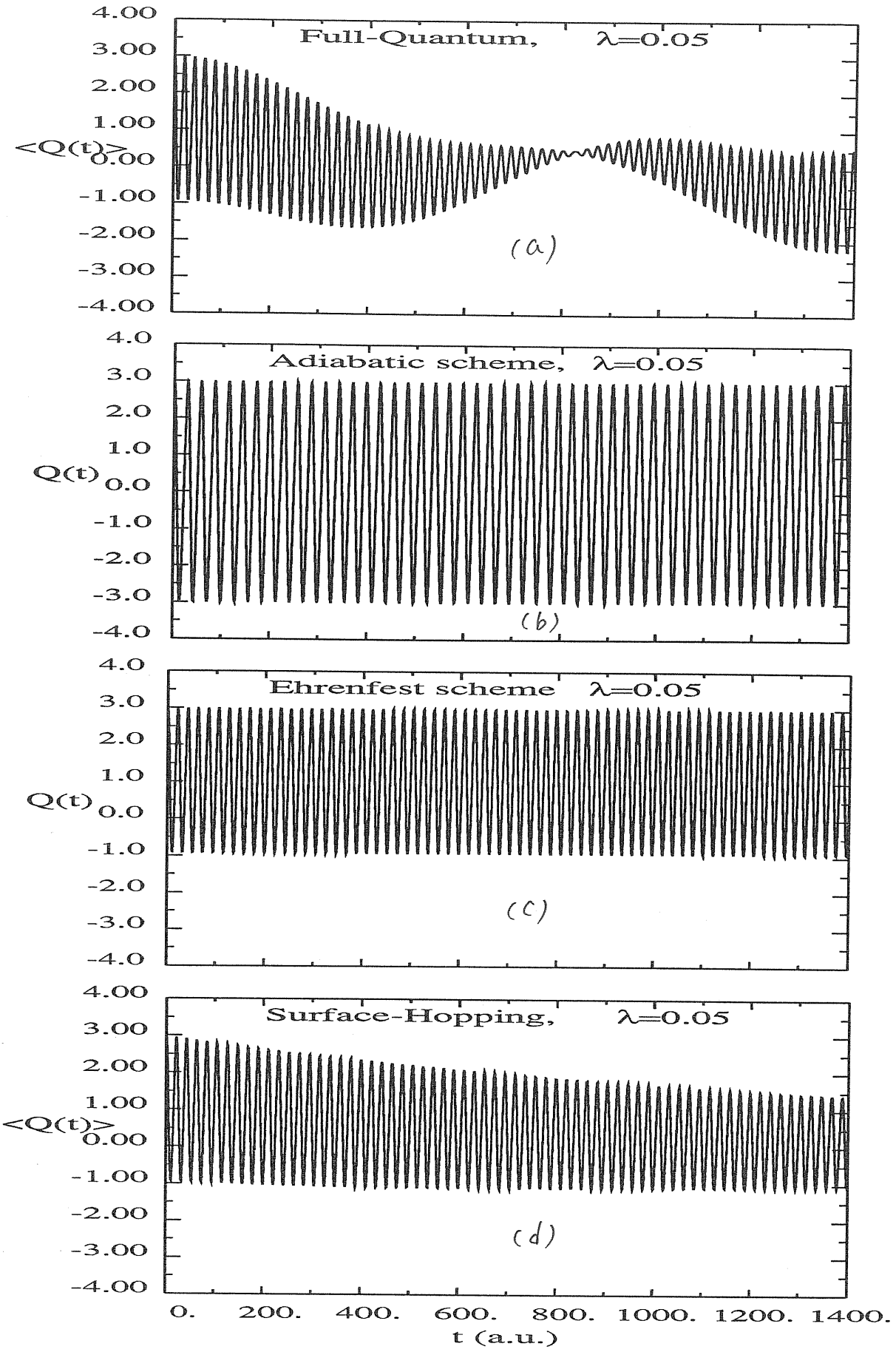

Fig.4 The time evolutions of Q at λ=0.05 for the four schemes, i.e. full quantum, adiabatic, Ehrenfest and surface hopping respectively, where <Q> in (a) is the expectation and <Q> in (d) is the value of Monte-Carlo averaging.

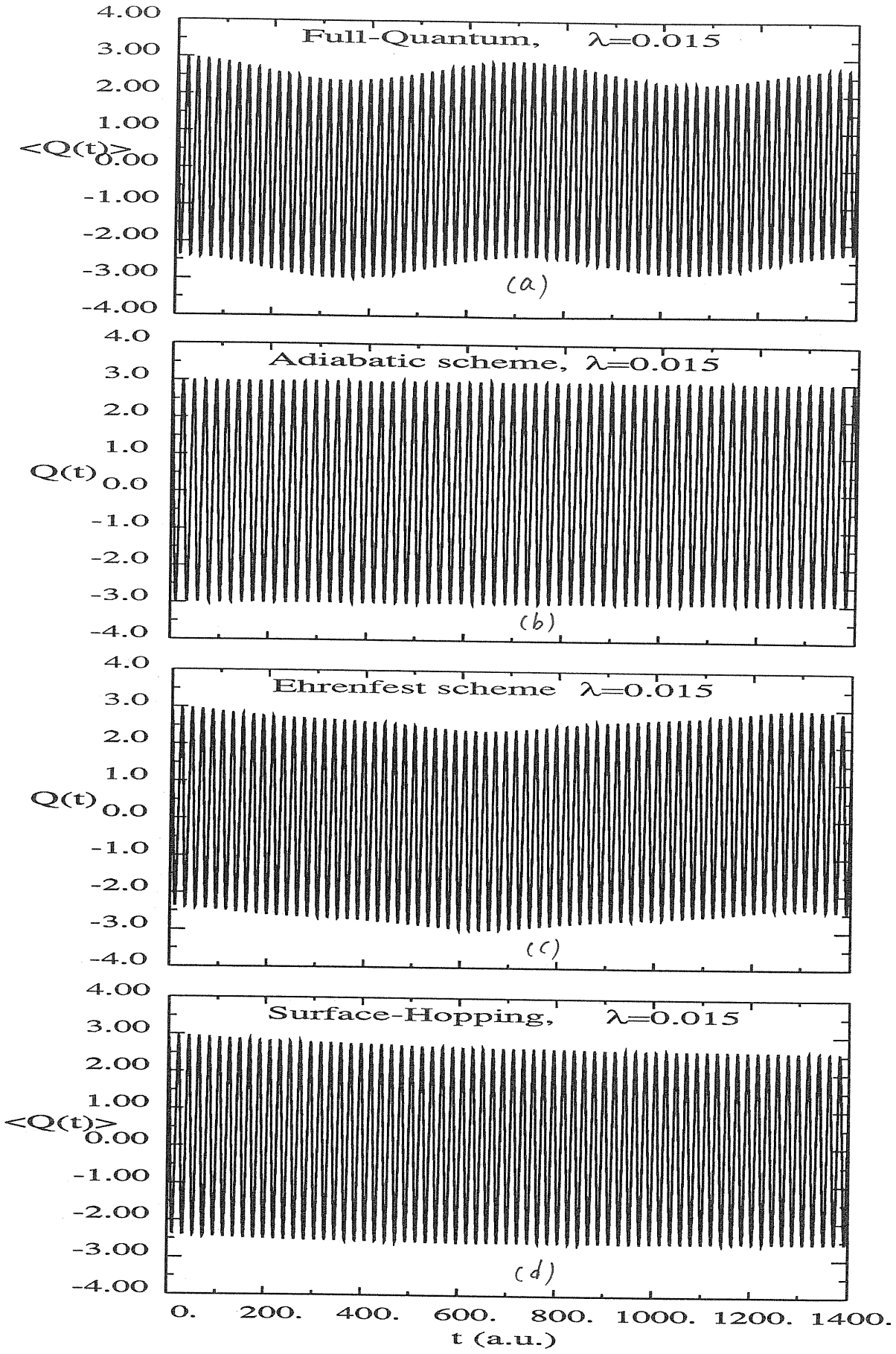

Fig.5 The time evolutions of Q at λ=0.015 for the four schemes, i.e. full quantum, adiabatic, Ehrenfest and surface hopping respectively, where <Q> in (a) is the expectation and <Q> in (d) is the value of Monte-Carlo averaging.

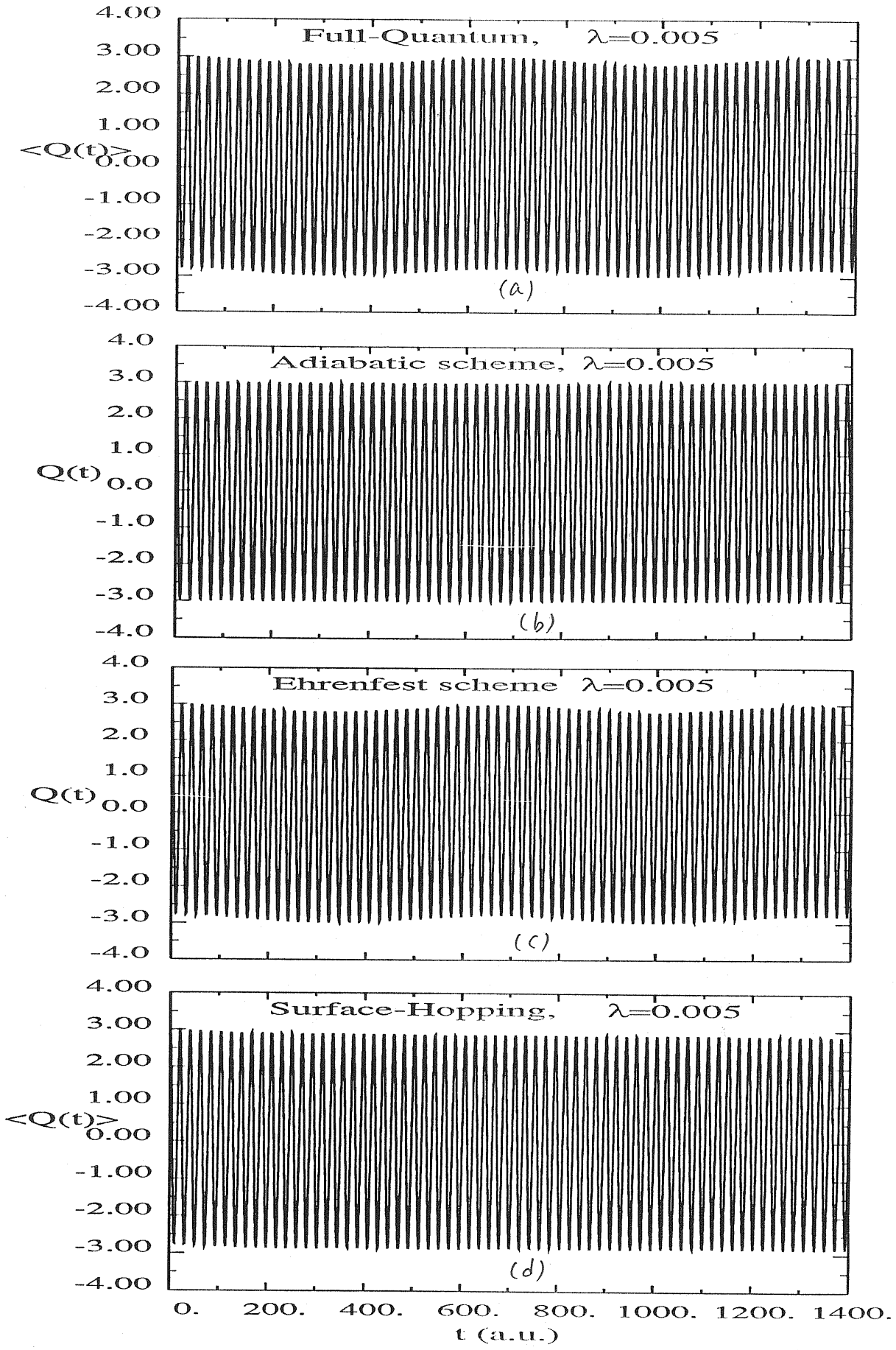

Fig.6 The time evolutions of Q at λ=0.005 for the four schemes, i.e. full quantum, adiabatic, Ehrenfest and surface hopping respectively, where <Q> in (a) is the expectation and <Q> in (d) is the value of Monte-Carlo averaging.

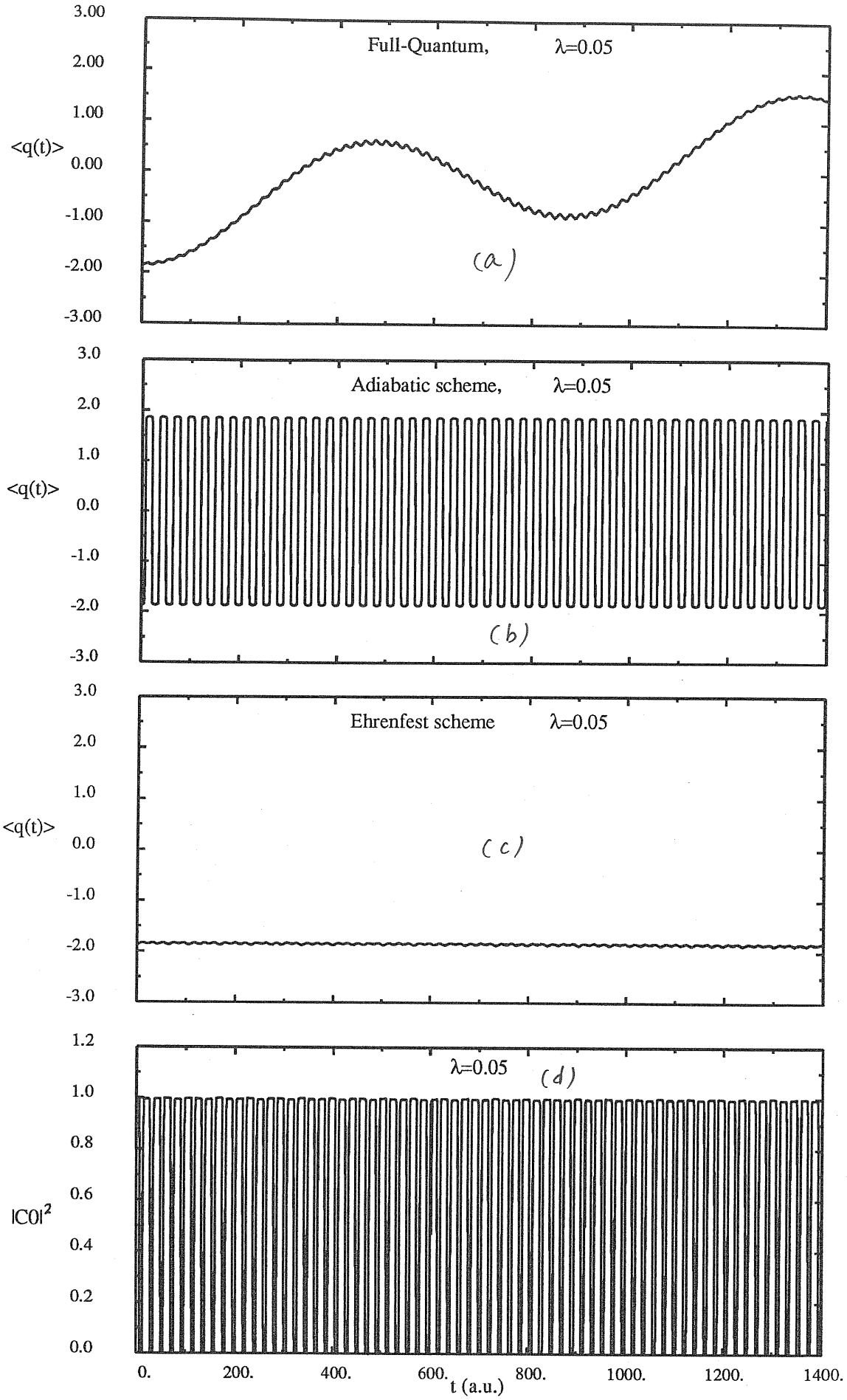

Fig.7 The time evolutions of the expectation <q> at $\lambda=0.05$ are given in (a), (b) and (c) for full quantum, adiabatic and Ehrenfest schemes respectively. The probability $|c0|^2$ of finding the "electron" in the instantaneous ground state of h(q;Q) in Ehrenfest scheme is plotted in (d).

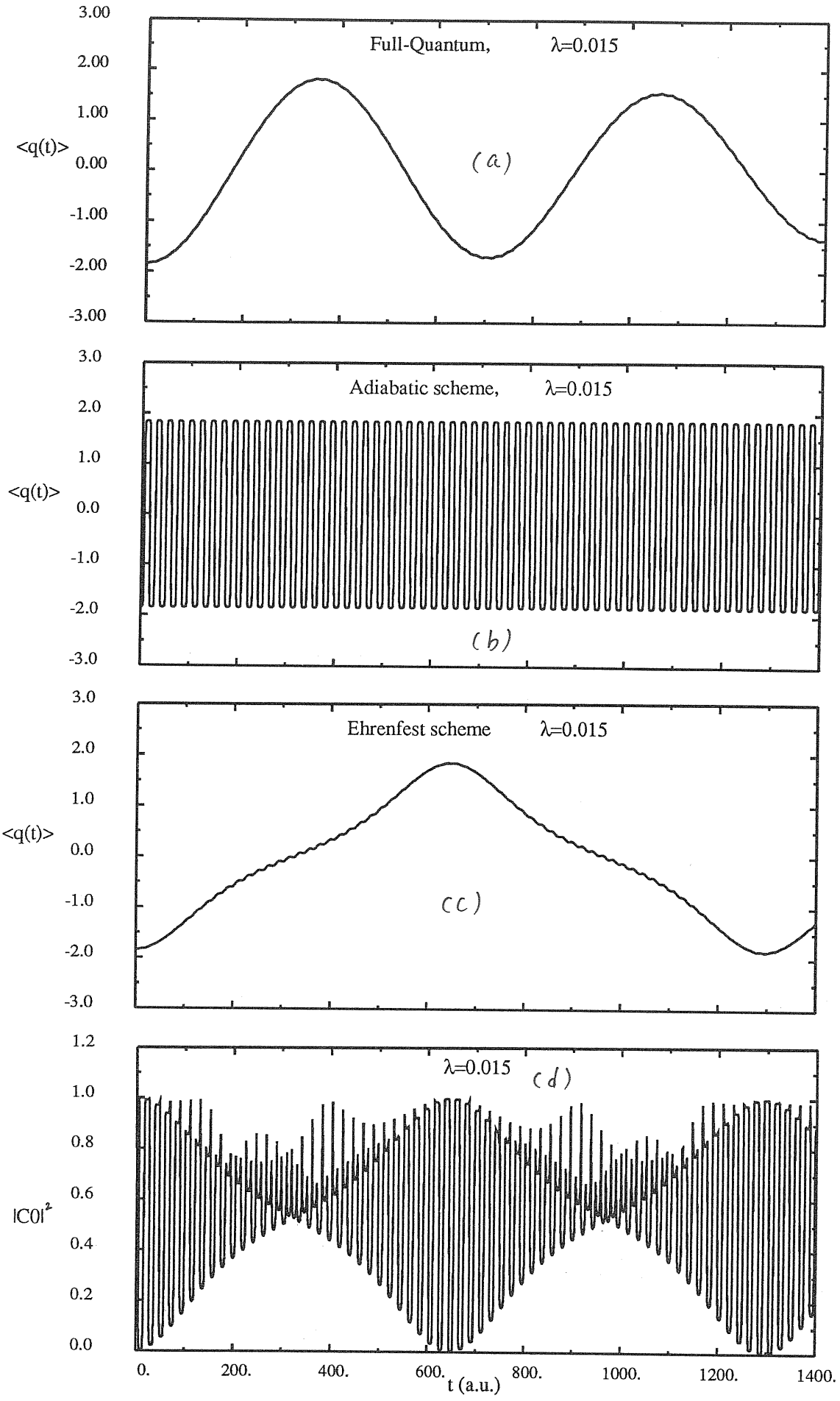

Fig.8 The time evolutions of the expectation <q> at λ=0.015 are given in (a), (b) and (c) for full quantum, adiabatic and Ehrenfest schemes respectively. The probability $|c0|^2$ of finding the "electron" in the instantaneous ground state of h(q;Q) in Ehrenfest scheme is plotted in (d).

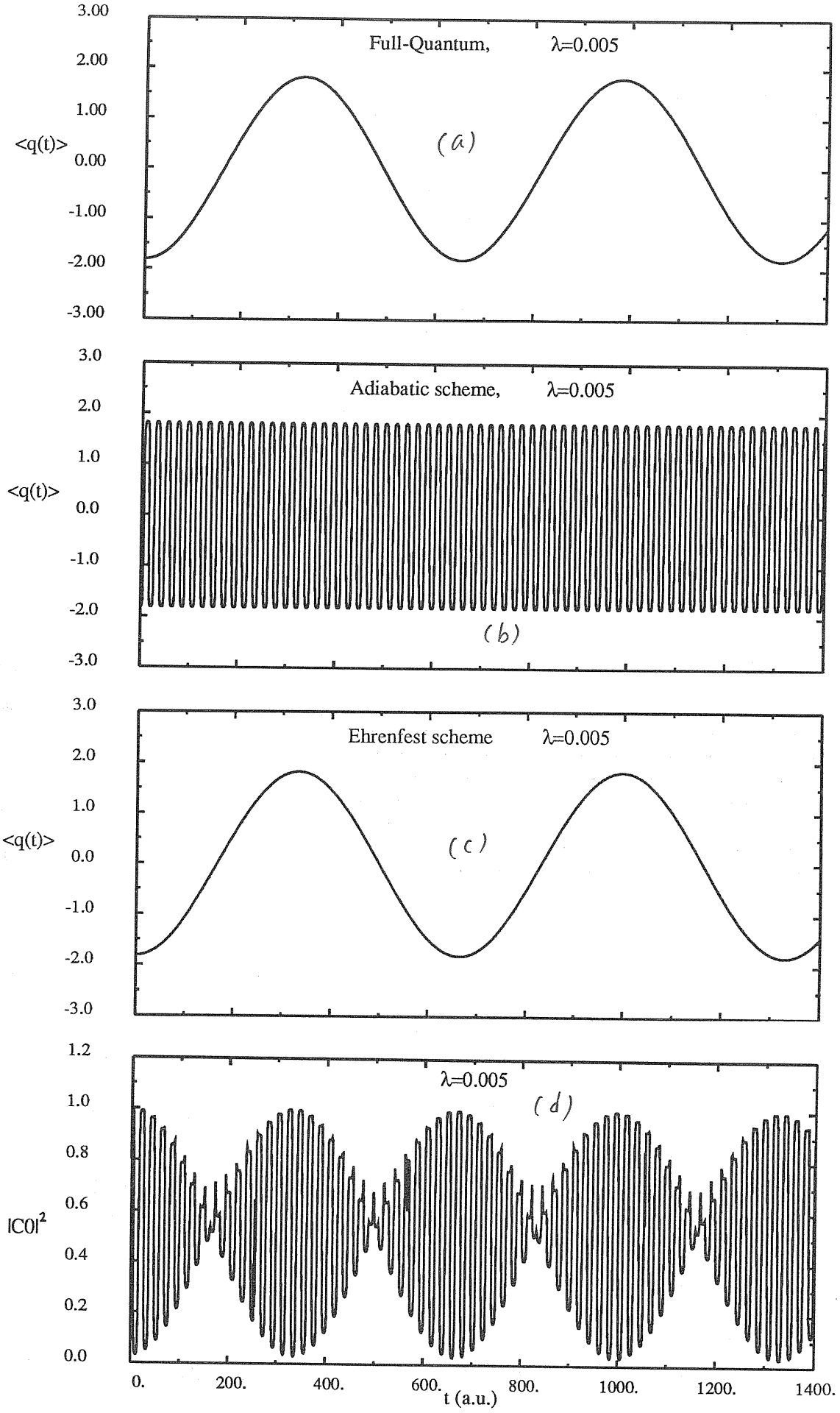

Fig.9 The time evolutions of the expectation <q> at λ=0.005 are given in (a), (b) and (c) for full quantum, adiabatic and Ehrenfest schemes respectively. The probability $|c0|^2$ of finding the "electron" in the instantaneous ground state of h(q;Q) in Ehrenfest scheme is plotted in (d).

from Q-subsystem to q-subsystem. The <Q>'s for the rest coupling cases moves as an anharmonic oscillator with a frequency ω_0. But their envelope change with the same period as the respective <q>'s. Whereas the <q(t)>'s for the three values of λ vibrate according to the periods given in Table3.1 though there are small fluctuations. This coincides with the qualitative description by Leggett and co-workers[Leg87], although their quantity studied is $P(t)=P_R-P_L$ (where $P_R(P_L)$ is the probability of finding the system in the right(left) well) rather than <q> here.

IV. Adiabatic Treatment

In this treatment, we adopt the Born-Oppenheimer (BO) adiabatic approximation and constrain the q-subsystem to stay in the ground state all the time.

a. Born-Oppenheimer Adiabatic Approximation[Bor27]

The Schrodinger equation of a system composed by electrons and nuclei is

$$H\Psi = E\Psi \qquad (4.1)$$

where the total Hamiltonian can be written as

$$H(\mathbf{q},\mathbf{Q}) = T_q + T_N + V(\mathbf{q},\mathbf{Q}) = h(\mathbf{q};\mathbf{Q}) + T_N \qquad (4.2)$$

Here, T_q and T_N are the kinetic energy operators for electrons and the nuclei respectively. V includes the various contributions to the potential energy. The electronic and nuclear coordinates are $\mathbf{q}$, $\mathbf{Q}$ and their corresponding momenta $\mathbf{p}$, $\mathbf{P}$. The coordinates $\mathbf{Q}$ act as parameters in the electronic Hamiltonian $h(\mathbf{q};\mathbf{Q})$.

In the BO approximation, one writes an approximate total eigenfuction of H as a simple product

$$\Psi(\mathbf{q},\mathbf{Q}) = \sum_i \varphi_i(\mathbf{q};\mathbf{Q})\chi_i(\mathbf{Q}) \qquad (4.3)$$

where $\varphi_i(\mathbf{q};\mathbf{Q})$ satisfies

$$h(\mathbf{q};\mathbf{Q})\,\varphi_i(\mathbf{q};\mathbf{Q}) = \varepsilon_i(\mathbf{Q})\varphi_i(\mathbf{q};\mathbf{Q}) \qquad (4.4)$$

where $\mathbf{Q}$ is a parameter.

Substituding Eq. (4.3) into Eq. (4.1), multiplying both sides by $\varphi_j^*(\mathbf{q};\mathbf{Q})$ and integrating over $\mathbf{q}$, we get

$$(T_N + \varepsilon_j(\mathbf{Q}) - E)\chi_j(\mathbf{Q}) = -\sum_{i\neq j}\sum_\nu \frac{1}{M_\nu}\langle\varphi_j|P_\nu\varphi_i\rangle . P_\nu\chi_i(\mathbf{Q}) - \sum_i\sum_\nu\langle\varphi_j|T_N\varphi_i\rangle\chi_i(\mathbf{Q}) \qquad (4.5)$$

Here, we have used the explicit expression for T_N

$$T_N = \sum_\nu \frac{P_\nu^2}{2M_\nu} \qquad (4.6)$$

M_ν being the mass of the ν-th ion.

In Eq. (4.5), the $\varepsilon_j(\mathbf{Q})$'s are the effective potential energy

surfaces that govern nuclear motion. The terms on the right hand side can promote transitions between potential energy surfaces, so we call them nonadiabatic interactions. Of these terms, the first is usually the dominant one[Tul75]. The nonadiabatic transition probability η was estimated[Mes65] as about

$$\eta \simeq (\frac{m}{M})^2 \frac{t_N}{\Delta}$$

where m and M are the electronic and nuclear masses respectively, t_N is the kinetic energy of the nuclei, Δ is the electronic level difference. Hence on one hand, If the tipical ionic freqencies are much smaller than the electronic level gaps, the nonadiabatic interaction is very weak and thus these terms can be neglected. On the other hand, the small ratio of the electronic and nuclear masses also makes these terms less important (this point is not stressed in the present thesis). In this case, the Schrodinger equation for the nuclei takes the simple form

$$(T_N + \varepsilon_j(Q) - E)\ \chi_j(Q) = 0 \qquad (4.7)$$

This means that the nuclei move in an effective potential surface which is the electronic energy for the relevant state (the interaction between nuclei has been included in ε_j)

b. Application to Our Model System

Using the BO separation, the Schrodinger equation for the model described in Sec.III splits into two one-dimensional Schrodinger equations

$$[-\frac{1}{2}\frac{d^2}{dq^2} + V_e(q) + V_c(q;Q)]\ \varphi_i(q;Q) = \varepsilon_i(Q)\varphi_i(q;Q) \qquad (4.8)$$

$$[-\frac{1}{2}\frac{d^2}{dQ^2} + V_I(Q) + \varepsilon_i(Q)]\ \chi_i(Q) = E\chi_i(Q) \qquad (4.9)$$

We now adopt a classical approximation for the Q-subsystem and hence discribe it in terms of its coordinate Q. The equations of motion (4.8)-(4.9) for our system thus become

$$[-\frac{1}{2}\frac{d^2}{dQ^2} + V_e(q) + V_c(q;Q)]\varphi_i(q;Q) = \varepsilon_i(Q)\varphi_i(q;Q) \qquad (4.8)$$

$$\ddot{Q} = -\frac{dV_I}{dQ} - \frac{d\varepsilon_i(Q)}{dQ} \qquad (4.10)$$

The set of Eqs.(4.8) and (4.10) state that at each instant the "electronic" system is in the i-th eigenstate corresponding to the "ionic" configuration Q, and at the same time the ionic system moves on the potential surface corresponding to the i-th electronic state.

c. Method of solution

Since Eq.(4.8) is an ordinary differential equation with asymptotic behavior $\varphi(q\to\pm\infty)\to 0$, it is very easy to solve it numerically by employing the Runge-Kutta method. In this method, the second order differential equation is divided into two first order equations.

$$\frac{d\varphi}{dq} = f(q) \qquad (4.11)$$

$$\frac{df}{dq} = 2[V_e(q) + V_c(q;Q) - \varepsilon_i]\varphi_i \qquad (4.12)$$

Starting from one point far enough from the origin that the function f and φ_i are there very small, one can use the Runge-Kutta single step method to calculate the function point by point. In the eigenvalue problem, we start from both a left and a right far point and calculate the function rightwards and leftwards respectively. At one appropriate matching point, the Wronskian determinant

$$\begin{vmatrix} \varphi_i^l & \varphi_i^r \\ f^l & f^r \end{vmatrix} \qquad (4.13)$$

should vanish when ε_i in Eq.(4.14) happens to be an eigenvalue of Eq.(4.8). In our model, the starting points are chosen at q= 5.0 where the normalized wavefunctions are very small ($\sim 10^{-6}$-10^{-7}). These

are represented on a mesh of 1024 points, making the numerical error $< 10^{-10}$.

Calculation of the first term on the right hand side of Eq.(4.10) is straightforward. The second term can be obtained using the Hellman-Feynman theorem

$$\frac{\partial \mathcal{E}_i}{\partial Q} = \langle \varphi_i | \frac{\partial V_I(\mathbf{r};Q)}{\partial Q} | \varphi_i \rangle \qquad (4.14)$$

Numerical integration of Eq.(4.10) is performed by the Verlet algorithm[Ver67]. This consists in approximating the time derivative using a finite difference method with time step Δt. More explicitly Eq(4.10) is solved using

$$Q(t+\Delta t) = 2Q(t) - Q(t-\Delta t) - (\Delta t)^2 \left[\frac{dV_I}{dQ} + \frac{d\mathcal{E}_i}{dQ}\right] \qquad (4.15)$$

The error is of order $O(\Delta t^4)$. The time step Δt in our calculation is 0.01 a.u.. With this Δt, the total energy

$$E = \frac{1}{2}\dot{Q}^2 + \langle \varphi_i | h | \varphi_i \rangle + V_I \qquad (4.16)$$

is conserved with a relative error of 10^{-4} during a run of about 10^5 time steps.

Since this is an adiabatic treatment, any transition is forbidden. In particular we enforce the "electron" to be on the ground state(i=0) all the time.

d. Results and Discussion

The Figs.4b, 5b, and 6b show the time evolution of the oscillator Q for three different values of the coupling constant. Comparing these results with those given by the full quantum calculation it seems that the disagreement is very sharp for all values of the coupling constant. The reason of such a disagreement is obviously that we are forcing the electronic system to be on the ground state, whereas electronic transitions to the 1st excited state can by no means be ignored when Δ becomes of the order or

smaller than the oscillator frequency. It is obvious in the strong coupling case that this adiabatic description gives rise to a time delay of Q(t). The reason is that the force from the q-quantum system in the ground state (the second term in Eq.(4.12)) is always against the restoring force of the oscillator.

The expectation values of q

$$\langle q(t) \rangle = \langle \varphi_0(q;Q(t)) | q | \varphi_0(q;Q(t)) \rangle \qquad (4.17)$$

are shown in Figs.7b, 8b, and 9b. We remark that in contrast to the full quantum results, these values have the same period as the Q's because <q> has an one to one correspondence to Q in this treatment.

V. Ehrenfest Treatment [Sel87]

a. Equations of Motion

Since it depends parametrically on Q while Q varies with time evolution, the $h(q;Q)$ in Eq.(4.4) is time-dependent. Alternatively, Eq.(4.4) can be replaced with the time-dependent Schrodinger equation

$$i\frac{\partial\Phi(q,t)}{\partial t} = h(q;Q(t))\Phi(q,t),\quad \Phi(q,t_0)=\varphi(q;Q(t_0)) \qquad (5.1)$$

where t_0 is a given initial time. We use instead the same equations as (4.10) + (4.14) to describe the motion of Q

$$\ddot{Q} = -\frac{dV_I}{dQ} - \int dq\,|\Phi(q,t;Q)|^2\frac{\partial V_c(q;Q)}{\partial Q}\,. \qquad (5.2)$$

The justification of Eqs. (5.1) and (5.2) has been given in the literature[Del72]. These equations lead to conservation of the energy of the system

$$\frac{d}{dt}\left[\frac{1}{2}\dot{Q}^2 + V_I(Q) + \langle\Phi|h|\Phi\rangle\right] = 0\,. \qquad (5.3)$$

For adiabatic motion Eq.(5.1) is equivalent to Eq.(4.4). Since the time variation of $h(q;Q(t))$ is usually so small with respect to the electronic energy gap Δ that no transition is induced, $\Phi(q,t)$ coincides with $\varphi_0(q;Q(t))$ except for a phase factor. Sometimes, people use Eq.(5.1) rather than (4.4) simply due to computational convenience. When Δ becomes of the order of the tipical ionic frequencies, $\Phi(q,t)$ can deviate substantially from $\varphi_0(q;Q(t))$, thus indicating the occurence of an electronic transition. This does not mean however that the set of Eqs.(5.1)-(5.2) is capable to describe nonadiabatic motion, since in this case the assumption of a single, well-defined classical trajec-

tory for the ion (Eq.(5.2)) breaks down. Nevertheless we still employ them to observe their validity by comparing their results with the exact ones.

b. Method of solution

The method of solution for eq.(5.2) is the same described in section IV for the corresponding Eq.(4.10). The main issue is to solve eq.(5.1). In our numerical procedure, $\Phi(q,t+\Delta t)$ is obtained from $\Phi(q,t)$ as

$$\Phi(q,t=\Delta t)=e^{-i\int_t^{t+\Delta t} h(t')\,dt'}\cdot\Phi(q,t)$$

$$\simeq e^{-iV\Delta t/2}\cdot e^{-iT_q\Delta t}\cdot e^{-iV\Delta t/2}\cdot\Phi(q,t)+O(\Delta t^3) \qquad (5.4)$$

where $V=V_e+V_c$ and T_q is the kinetic operator for q. The matrix multiplication in Eq.(5.4) is performed by a Fast Fourier Transform (FFT) method[Fei82] which uses the fact that $e^{-iV\Delta t/2}$ is diagonal in real space while $e^{-iT_q\Delta t}$ is diagonal in reciprocal space. Since the use of Fourier Transform techniques require periodic boundary conditions, we choose a region for q from -5 to 5 and repeat it periodically. The wavefunction Φ is here represented on a discrete mesh of 1024 points. The finite size of our region does not influence our results because the potential at the boundaries is so high that the wavefunctions of interest and their first order derivatives are practically zero. The time interval Δt is 0.01 a.u. to conserve the total energy to better than 10^{-4} over the whole evolution($\sim 10^5\Delta t$). Every 100 Δt we also calculate the ground state φ_o of the instantaneous hamiltonian in order to obtain the occupation number

$$|C0|^2=|\langle\Phi|\varphi_o\rangle|^2 \,. \qquad (5.5)$$

c. Results and Discussion

Three calculations corresponding to three different λ values, 0.05, 0.015 and 0.005, have been done. The time evolutions of Q and the expectation values of q are showed in Figs.4c, 5c, 6c, 7c, 8c and 9c respectively. The Q(t)'s oscillate with the same frequency as that of the full quantum case. For the strong coupling (λ=0.05), the oscillator moves on the lower potential surface when Q<0 but on the upper surface when Q>0. This implies that the trajectory always hops at the crossing point Q . For the same coupling case, the <q> (see Fig.7c) is about -1.8 on the whole time scale except for a small fluctuation. This indicates that the particle always locates in the left well of the double-well, i.e. no tunneling occurs. This situation changes in the intermediate and weak coupling cases (see Fig.8c, 9c). The values of $|c0|^2$ (Figs.7d, 8d and 9d) tell us that the motion is no longer adiabatic. But it is interesting to notice from Figs.6c and 9c that the Ehrenfest scheme gives a good agreement with the full quantum ones for the weak coupling case. The particle tunnels back and forth in a cosine function with the frequency Δ. This behaviour also agrees with that described by Leggett[Let87].

The results worsen with increasing λ value. For the intermediate coupling case, the particle does tunnel but neither in a simple cosine form nor with the frequency Δ. Its tunneling frequency is about half of the full quantum one. So is the envelope of Q. For the strong coupling case, the results qualitatively disagree with the full quantum ones. This is the consequence of breaking down of BO approximation.

The reason why the Ehrenfest scheme gives a good description for the weak coupling case is not yet very clear. One possible explanation is that the terms we have neglected on the right hand of eq.(4.5) do vanish because of the weak dependence on Q of φ_i's. The two potential surfaces in Fig.3a are almost parallel each other, so the restoring forces for the oscillator are in the same direction at any Q point. Hence the trajectories along the two potential surfaces do not diviate appreciably. On the other hand, in Figs. 3b and 3c, the two surfaces differ somehow. The two forces are opposite at some Q points.

VI. Surface Hopping Treatment

a. Surface-Hopping method

In the study of the dynamics of molecular collisions, Tully and co-workers[Tul71] have developed a method to treat nonadiabatic collisions called the "Trajectory Surface Hopping Approach"(SH). The method has been quite successful in general cases and therefore become quite popular. Here we give a short introduction to it.

Within the Born-Oppenheimer approximation, the nuclear motion can be described by classical mechanics. The motion is governed by the effective potential energy surfaces $\varepsilon_i(\mathbf{Q})$, just like those in Eq.(4.7). The different electronic levels i correspond to different potential surfaces for the nuclei. It is however possible that for some configurations, which are called crossing points, two or more such adiabatic potential energy surfaces approach each other closely, and then nonadiabatic transitions occur with high probability. In the SH model, a nonadiabatic transition is represented by a hop of the classical particles $\mathbf{Q}$ from one adiabatic potential surface to another. A method for computing the hopping probability should then be selected. In the one-dimensional case, the simplest is the Landau and Zener(LZ) method[Lan65]. Every time the trajectory of the nuclei pass through a crossing point, it will split according to the given transition probability. Both of these branches might reach a second crossing point and split again, and so forth, so that a given set of initial condi-

tions can result in a trajectory which contains a great many branches. The final result is the average over all such trajectories starting from a same set of initial conditions. An alternative way to average over different trajectories using a Monte Carlo procedure[Tul71] is described below. This approach has achieved good results both in molecular collisions [Tul71] and in dissipative system [Ray87]. However, this method has sacrificed any information about electrons.

b. Application to Our Model

We use the classical equation of motion (4.10) to describe Q. The crossing point in our model is chosen at $Q_0=0$. When Q crosses Q_0, the hopping probability for the system to change electronic state is calculated using the Landau, Zener and Stueckelberg[Tul75] formula

$$P_{LZ}= \exp[- \frac{2\pi \Delta^2}{v|F_1 - F_2|}] \qquad (6.1)$$

where Δ is the gap, v the velocity of the oscillator and F_1 and F_2 the slopes of the diabatic potentials (i.e. surfaces with $\Delta =0$) at the crossing point for the surface 0 and 1 respectively. At this point a kind of Monte Carlo procedure is used, in the same way as Tully *et al.* A random number R is generated. If P_{LZ} is larger than R, a hopping occurs, otherwise Q keeps moving on the same potential surface. To conserve the total energy, the velocity must be adjusted at each hopping. In this way, we get one trajectory. Repeating this process a great number of times, we get many different trajectories. The final results are obtained by averaging over the different trajectories.

c. Results and Discussion

The Monte Carlo averaged results for Q have been obtained as usual for three values of λ. The number of trajectories (3000 for λ=0.005,0.015; 10000 for λ=0.05) has been checked to be enough for convergence. For the strong coupling case, the surface hopping results give some improvement to both the adiabatic and the Ehrenfest schemes. For this λ value, the trajectory at the crossing point always hops in the Ehrenfest scheme but always stays at the lower surface in the adiabatic one. So the surface hopping scheme does some intermediate between these two extreme cases, in the sense that sometimes there is a jump from a potential surface to the other, and sometimes there is not. The improvement is noticeable. For the first few periods, the present results are quite good (see Fig.4d). But on a longer time scale, they are different from the exact ones: although there is still some amplitude damping, the envelop does not oscillate as in the exact results. The amplitude damping can be understood as more and more trajectories move on the upper potential surface with time evolution. Because at the crossing point the velocity for the upper surface is smaller due to the energy conservation, the probability P for hopping 0→1 is larger than that for hopping 1-0. We also remark that the surface hopping results worsen with decreasing λ (see Figs.4d, 5d and 6d). The reason is that as λ decrease it becomes more and more difficult to determine at which point the crossing should occur. In our calculation, we always chose Q =0 as the crossing point. Unfortunately, the information about the q-subsystem has been lost in this model.

VII. Conclusion

In this work we have observed the time evolution for a coupled system consisting of a two-state subsystem ("electron") and an oscillator ("ion"). The time evolution has been studied with different schemes, namely adiabatic, Ehrenfest and the trajectory surface hopping(TSH), whose validity has been checked against a full quantum mechanical evolution. We have chosen the particular, but very interesting case where the electronic subsystem has two very closely separated levels (tunneling levels), where the adiabatic scheme is not expected to apply.

Comparing the results obtained by the adiabatic, Ehrenfest and TSH schemes with the exact quantum-mechanical ones, we first of all confirm that the adiabatic treatment gives totally wrong results.

Both the TSH and Ehrenfest scheme may be either good or bad, depending on the physical situation. The TSH scheme works best in the strong coupling case where the adiabatic potential energy surfaces have isolated near-crossing points (also called Landau-Zener region) and keep well apart most of the time. In this region, the Ehrenfest scheme fails. It should be noted however that the TSH scheme can only give a description of the nuclear motion without any electronic information.

In contrast to TSH, the Ehrenfest evolution gives a very good agreement with the true evolution in the weak coupling case, where the potential energy surface are nearly

parallel and hence have no well-defined near-crossing points. If the potential energy surfaces keep roughly parallel to each other, and in addition, are very far apart in energy, then both the adiabatic and Ehrenfest schemes work equally well. In our case, however, tunneling implies very closely separated surfaces (Fig.3a), and for this case only Ehrenfest scheme works well.

One final comment is that in the strong-coupling situation one may speak of electron "tunneling" between two self-trapped potential wells. Because this tunneling is well localized near Q=0 (surface near-crossing point, Fig.3c), the Landau-Zener treatment of TSH works well for this case. No such well-defined tunneling is identifiable in weak coupling (Fig.3a), which explains why TSH fails in this case.

Summarizing: when a fast and a slow degrees of freedom are coupled together, their joint quantum mechanical evolution can be given a satisfactory approximate description even in those cases where the usual adiabatic approximation fails. In the particular case where the electronic subsystem has two very near tunneling levels, we have found that the Ehrenfest scheme works very well for weak coupling, whereas the TSH scheme works well for strong coupling. Nevertheless, the TSH scheme is clearly incomplete, since all information about the fast degree of freedom is lost. Work is in progress to find alternative scheme that could fill up this deficiency.

Reference

[Bor27] M. Born & J. R. Oppenheimer,
Zur Quantentheoric der Molekeln. Ann. der Phys. 84
p457-484 (1927)
or M. Born & K. Huang,
Dynamical Theory of Crystal Lattices
(Oxford University, New York, 1956), Appendix.

[Car86] R. Car & M. Parrinello,
Phys. Rev. Lett. 55, p2471 (1986)

[Del72] J. B. Delos & W. R. Thorson,
Phys. Rev. A6, p720 (1972)

[Fei82] M. D. Feit, J. A. Fleck and A. Steiger,
J. Comp. Phys. 47, p412 (1982)

[Gar77] B. S. Garbow, J. M. Boyle, J. J. Dongarra & C. B. Moler,
"Matrix Eigensystem Routines -- EISPACK Guide Extension"
Springer-Verlag (1977)

[Gra84] R. Graham & M. Hohnerbach,
Z. Phys. B57, p233 (1984)
and the reference therein.

[Her63] F. Herman & S. Skillman
Atomic Structure Calculations
(Englewood Cliffs, N.J. Prentice-Hall, 1963)

[Lan65] L. D. Landau & E. M. Lifshitz
Quantum Mechanics (non-relativistic theory)
2nd ed. p322, Peramon Press (1965)

[Leg87] A. J. Leggett, S. Chakravarty, A. T. Dorsey,
Matthew P. A. Fisher, Anupam Garg & W. Zwerger
Rev. Mod. Phys. 59, p1 (1987)

[Mes65] A. Messiah

"Quantum Mechanics" vol. II, p787
North-Holland Company, 1965

[Ray87] Raymond E. Cline, Jr. & Peter G. Wolynes,
J. Chem. Phys. 86, p3836 (1987)

[Sch55] C. I. Schiff,
"Quantum Mechanics", p67
2nd ed. McGraw-Hill Book Company. (1955)

[Sel87] A. Selloni, P. Carnevali, R. Car & M. Parrinello,
Phys. Rev. Lett. 59, p9823 (1987)

[Tul71] J. C. Tully & R. K. Proston,
J. Chem. Phys. 55, p562 (1971)

[Tul75] J. C. Tully
in "Dynamics of Molecular Collisions" Part B, Ch.5
edited by William H. Miller
Plenum Press, 1975

[Ver67] L. Verlet,
Phys. Rev. 159, p98 (1967)